Digitisation of bamboo culms for structural applications

Rodolfo Lorenzo[1*] and Leonel Mimendi[1]
[1]Department of Civil, Environmental and Geomatic Engineering, University College London, London, UK
*Corresponding author: Rodolfo Lorenzo r.lorenzo@ucl.ac.uk

Abstract

Reducing the negative environmental impact caused by the intensive manufacturing of industrialised building materials and components requires the adoption of alternative sustainable resources and the development of appropriate procedures to encourage their use in the construction industry. Bamboo in its natural form (culms or poles) is one of the most promising non-conventional sustainable building materials, endemic to most developing countries where high demand for building materials will be driven by the large-scale urbanisation predicted for the coming decades. The use of bamboo poles as structural elements poses multiple challenges starting with the need to define their inherent geometric variability to enable their inclusion in formal design and fabrication processes. This paper describes the details of a non-destructive 3D scanning and modelling workflow developed to capture and process the relevant digital information that describes the geometric properties of bamboo poles. The digitisation of over 230 poles with a combined length of 500 m was carried out confirming the accuracy of the generated geometric models. Also, a small reciprocal frame prototype was successfully developed based on the geometric information extracted from a 3D model of the structure incorporating the digitised poles. The effective digitisation of bamboo poles and its integration into modern platforms can provide the construction industry with the necessary support to design, build and maintain high quality structures that incorporate this sustainable and renewable resource.

Keywords: Bamboo; Sustainable building materials; Computer-aided design; Reverse engineering; Construction technology

1. Introduction

The construction sector is currently responsible for 40% of the greenhouse gas emissions in cities [1] due to the energy-intensive building materials developed during the last century for a very different world. Steel, concrete and aluminium, the three main construction materials, are already responsible for almost 50% of all industrial CO2 emissions worldwide with demand expected to double by 2050 [2]. Construction at this large scale will undoubtedly require the use of non-conventional renewable materials and the development of design and construction processes appropriate for these materials.

Bamboo in its natural form (culms or poles) is one of the most promising non-conventional sustainable building material endemic to most developing countries where large urbanisation is expected to take place. Studies on their biological and anatomical properties [3,4] have confirmed their potential as a renewable construction material, reaching heights of up to 30 m in a few months and full maturity in three to five years. It is estimated that the production of natural bamboo poles causes five times less harm to the environment compared to industrialised bamboo products [5]. Furthermore, the potential annual carbon sequestration for bamboo plantations is 4.30 tonnes/ha [6] which is comparable to the 3.2 to 10 tonnes/ha of tropical forests [7]. Out of the 1600 bamboo species in the world [8], over 100 species have been so far identified suitable for construction [9] and therefore capable of reducing the demand for industrialised building materials, while promoting economic activity in rural regions to reduce the current pressure on urbanised areas [10].

For all their qualities and potential, bamboo poles still need to overcome multiple technical and cultural barriers before they become an accepted alternative structural element. To achieve this, the construction industry must look beyond its traditional processes and the empirical know-how that bamboo construction currently relies on. Digital modelling, robotic fabrication and other advanced tools are revolutionising the built environment and thus it seems fitting to challenge the common misconception that bamboo culms and these advanced technologies are part of mutually exclusive realms. One of the main challenges posed by bamboo poles as structural elements is their inherent geometric variability which needs to be accurately quantified to enable their inclusion in formal design and fabrication processes.

Bamboo poles are tapered hollow tubes with transverse solid diaphragms spaced along their length. These diaphragms form part of the nodes of the culm identified by the characteristic circumferential growth scar on the bamboo surface (Figure 1). The challenges of using a natural building element with significant geometric variability in shape, taper and straightness were identified by Janssen [11] who suggested the use of average properties potentially suitable only for preliminary designs. Contrary to timber which can be sawn into standard shapes and sizes [12], standardised bamboo elements can only be produced splitting the tube wall into narrow strips which are then heavily processed into industrialised components with similar sustainability credentials as those of other manufactured elements [13].

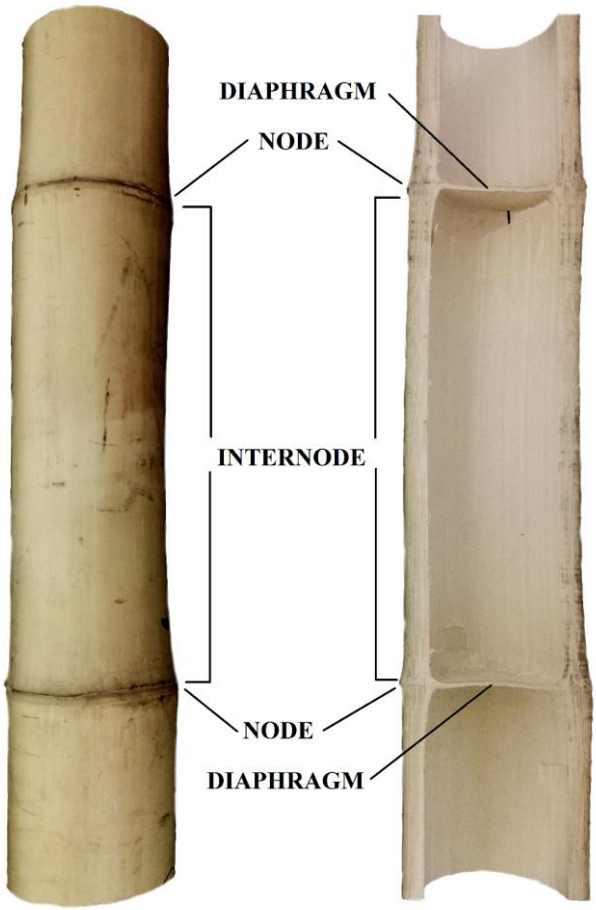

Figure 1. Main physical features of bamboo culm

Previous studies on the geometry of bamboo culms [14–16] have focused on studying its variability with the objective of establishing variational patterns from which conservative geometric estimates can be inferred. The applicability of these estimates as design parameters or as a grading system for bamboo poles [17,18] is relatively limited and can lead to overconservative guidelines due to the large geometric variability found across different species and even among a small sample of poles [19]. Other research [20,21] have focused on the study of the out-of-straightness of the pole's centroidal axis, designing methodologies to measure it and quantify its effect on their structural performance. These previous studies and the only international standard on structural bamboo ISO 22157-1-2004 [22], all rely on traditional manual tools and methods with significant limitations to accurately and efficiently capture the spatial geometric variability of organic objects such as bamboo poles.

The recent emergence of digital technologies and the rapid development of computer aided design (CAD) software has supported the emergence of multiple technologies in which the complex geometry of objects can be digitally captured and analysed [23]. Different non-destructive methodologies to capture complex shapes have been developed through the use of photographs [24,25], video-recording [26], laser sensors [27,28] and LED light projections [29,30] demonstrating the major advantages in speed and accuracy that these digital methods can offer compared with conventional analogue processes [31]. These modern technologies are becoming increasingly accessible including the numerous proprietary and open source software packages [32–34] available to process the captured raw data into basic 3D digital models. Several studies have focused on developing methodologies to further develop these basic 3D representations into more practical digital models for architectural [35], mechanical [36,37] and structural applications [38,39] that can be incorporated into Building Information Modelling (BIM) platforms [40,41] to support the development of infrastructure projects from design to operation and decommissioning.

This paper describes the details of a non-destructive 3D scanning and modelling workflow developed to capture and generate the relevant digital information that describes the geometric properties of bamboo poles. This workflow is based on the systematic scanning of individual bamboo poles from which a standard polygon mesh model [42] is generated. This mesh is subsequently transformed into a more flexible and manageable NURBS model [43] from which the fundamental geometric properties of bamboo poles are automatically extracted. This digitisation process is applied to the development of a full-scale prototype of a reciprocal frame system whose correct assembly fully relies on accurately quantifying the geometric properties of its constituent parts. This workflow lies at the core of the wider reverse engineering approach for bamboo poles proposed by Lorenzo et al [44] in which geometric digitisation and intensive, non-destructive mechanical testing of robotically-fabricated small clear samples can enable the global analysis of bamboo structures while building significant databases to increase our understanding of this inherently variable natural material. Moreover, 3D scanning, robotic fabrication and other new digital technologies can support a progressive structural design approach for bamboo poles based on digital modelling, parametric design, advanced simulations, rapid-

prototyping and experimental testing to support the design, analysis, optimisation, fabrication and management of high-quality and reliable bamboo structures.

2. Digitisation process

2.1. Scan subject and equipment

From a 3D scanning perspective, a bamboo pole can be described as a cylindrical slender element with a very small depth-to-span ratio. The internodal surface is smooth and relatively reflective without a distinctive texture or clear geometric features which are generally detrimental features for 3D scanning processes. On the contrary, the area around the bamboo nodes exhibit characteristic growth scars in the form of circumferential ridges and other imperfections (e.g. branch stubs) that provide the required texture and geometric features that facilitate the 3D scanning process (Figure 2). As a non-destructive process, the bamboo wall thickness is captured from both ends of the pole ensuring that these end sections lie within the central portion of the internodal region to guarantee an unrestricted view without interference from the nodal diaphragms. Figure 2 shows the cut end of a bamboo pole and the M5 socket head button screws used as reference markers between the physical poles and its scanned digital model. Each screw head is coated with a white liquid chalk marker prior to their insertion into predrilled holes at the sacrificial end internode of the pole approximately one diameter away from the last node. For identification purposes, a pair of screws are installed at the bottom of the pole and a single screw at the top.

Figure 2. End section of bamboo pole and scanning reference markers

Based on these general features, the required accuracy and a basic cost-benefit analysis, the equipment adopted for this project was an entry-level *Eva* scanner from Artec 3D [45]. This is a hand-held device that operates based on structured light sensor technology [40] with a resolution of up to 0.5mm and a 3D point accuracy of 0.1mm. The texture resolution is 1.3 mp and supports 24 bpp of colour. It projects a white LED structure light using flash bulbs with a maximum frame rate of 16 fps and an exposure time per frame of 0.0002 s. The scanning range of the device is 0.4 to 1.0 m with a linear field of view of 214 x 148 mm to 536 x 371 mm (height x width) respectively. The scanner is able to acquire a maximum of 2 million points per second.

The scanner was operated using a laptop Dell XPS 15 equipped with an Intel i7-6700HQ CPU @ 2.66GHz, 16GB of installed memory and a dedicated video card Nvidia GTX GeForce 960m with 4GB of memory. The raw data post-processing to obtain the polygon mesh of the scanned bamboo pole was carried out using Artec's proprietary software *Artec Studio 12* [45] in a work station Dell Precision with an Intel Xeon E5-1620v3 CPU @ 3.5GHz, 32GB of memory and a dedicated video card Nvidia Quadro K2200 with 4GB of memory.

2.2. 3D Scanning

The scanning workflow was developed based on the following requirements: i) portability for site use, ii) minimum file size & scanning/post-processing time and iii) sub-millimetre accuracy. Figure 3 shows the proposed scanning set-up in which individual bamboo poles are supported on a series of four V-head pipe stands with ball rollers which allow the pole to slide along and rotate about its longitudinal axis. The 3D scanner is mounted on a camera dolly and positioned on a workbench facing, and approximately

levelled with, the bamboo centreline. The lack of strong geometric features and texture in bamboo poles along with its relatively symmetric cylindrical shape requires careful consideration of the rate at which the scanner captures individual frames of data points to prevent it from losing track of the object. Also, each captured frame needs to be significantly overlapped with its adjacent frames to ensure their correct relative alignment as they are eventually merged into a single point cloud and processed into a polygon mesh.

Based on these considerations, the proposed scanning workflow involves the simultaneous longitudinal translation of the pole and rotation about its longitudinal axis as schematically shown in Figure 3. Adequate accuracy and resolution are obtained positioning the pole 700 mm away from the scanner which remains stationary as the pole is scanned in a helical pattern that ensures the horizontal and vertical overlap of individual frames. At the start and finish of the scanning process, when the ends of the pole are in the scanner's line of sight, the pole is held in position rotating it about its longitudinal axis for one full revolution after panning the scanner 45° around a semi-circular path to capture the cross section at the ends of the pole. This workflow ensures the continuous scan of each pole in one single scanning operation to improve the efficiency of the post-processing [46].

Even though the height of the scanner's field of view is larger than the diameter of the poles, the natural curvature of the bamboo surface effectively reduces this height to approximately half the pole's diameter so that only the central portion of the pole closest to the scanner can be captured in each individual frame. The height, *h*, of the captured frame was therefore conservatively assumed to be half the pole diameter, *D*, as shown in Figure 4, along with the sequence of frames captured during a full revolution and the corresponding translation of the pole. The relation between the scanner's frame rate and the speed of movement of the pole as it is being scanned is crucial to obtain the correct frame overlap to ensure an accurate result while minimising the scanning and post-processing time. Considering that the 3D scanner captures up to 2 million points per second and that the post-processing time increases exponentially after approximately 3000 frames, it was considered appropriate to limit the maximum number of captured frames per pole to 2000. Also, experimental trials showed that a rate of rotation of the pole of 3 seconds per full revolution ensured a smooth movement which prevented the scanner from losing track of the object. These trials also showed that a minimum horizontal and vertical overlap of 75% between adjacent frames guaranteed their correct alignment during post-processing. As shown in Figure 4, the critical vertical overlap (βh) occurs between sequential frames while the critical horizontal overlap (αw) takes place between the first (*frame 1*) and last frame (*frame n*) within one full revolution. Based on these considerations, the total number of captured frames per revolution is:

$$n = \frac{\pi D}{(1-\beta)h} = \frac{2\pi}{(1-0.75)} = 8\pi \ \ frames/rev$$

Considering a period, *T*, of 3 seconds per revolution, the angular velocity of the pole is:

$$\omega = \frac{2\pi}{3} \cong 2 \ rad/s$$

leading to a scanner frame rate of:

$$f = \frac{n\omega}{2\pi} = \frac{8\pi \times 2}{2\pi} = 8 \ fps$$

finally, the width, *w*, at the adopted 700 mm scanning distance is 260 mm which leads to the pole's translation speed:

$$v = \frac{(1-\alpha)w}{2\pi/\omega} = \frac{(1-0.75)260}{2\pi/2} \cong 20 \ mm/s$$

the maximum length of bamboo poles, *L*, is usually limited to 4 m due to transportation restrictions and so the longest scanning time is:

$$t = \frac{L}{v} = \frac{4000}{20} = 200 \ \ s/pole = 3 \min 20 s/pole$$

and the maximum number of scanned frames:

$$N = ft = 8 \times 200 = 1600 \ \ frames/pole$$

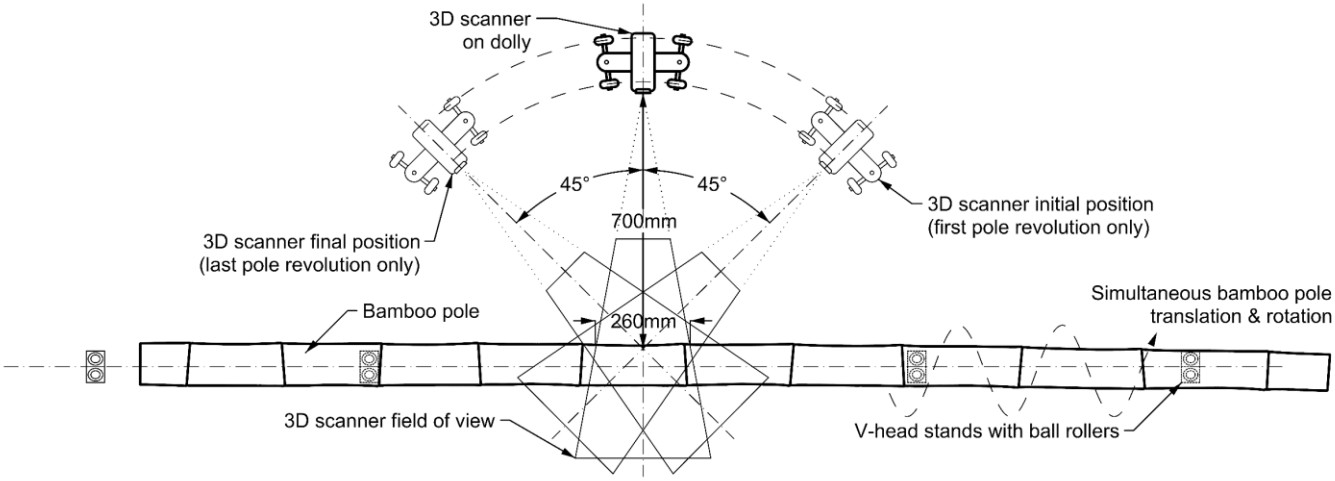

Figure 3. Schematic plan view representation of 3D scanning set-up

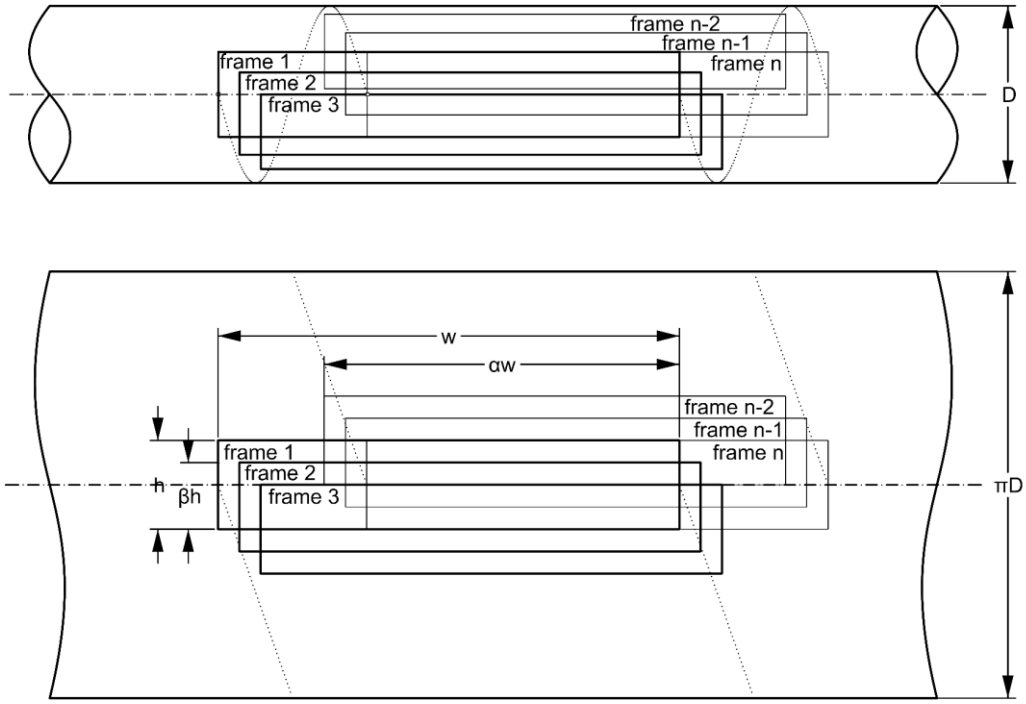

Figure 4. Sequence of scanned frames per revolution on an idealised cylindrical pole and its developed surface

The maximum number of scanned frames per pole is significantly less than the suggested limit of 2000-3000 frames and therefore ensures the efficient post-processing of the captured data.

The final scanning parameters, summarised in Table 1, are independent of the pole diameter and can deviate ±10% from their theoretical values without affecting the proposed workflow. The flexibility of this workflow to accommodate the natural geometric variability of bamboo is fundamental to facilitate its effective automation in an industrial setting with an average scanning time for a typical 4 m long pole of approximately 3 minutes.

Table 1. Recommended parameters for 3D scanning workflow

3D Scanner	Artec Eva
Scanning distance	700 mm
Bamboo angular speed (rad/s)	2 (or ≈ 3 s/rev)
Bamboo linear speed (mm/s)	20

2.3. Polygon mesh

A sample of the scanned raw data is shown in Figure 5 for a portion of a scanned bamboo pole. This data is processed with the software Artec Studio 12 [45] to obtain a single point cloud and subsequently a polygon mesh of the scanned object. Firstly, the point cloud is processed through the *Fine Registration* algorithm which aligns the captured frames based on both geometry and texture information. Within this algorithm there is a secondary *Loop_Closure* process to register frames not necessarily captured

in series, compensating for cumulative errors and highly recommended for hand-held devices. Secondly, the *Global Registration* algorithm converts all surface frames to a single coordinate system by matching the position of surface pairs also using geometry and texture information. Thirdly, an *Outlier Removal* algorithm removes all small surfaces (noise) not connected to the main surface. This process is based on a statistical algorithm that calculates the mean distances between each surface point and its neighbouring points. Distances greater than an interval of the standard-deviation multiplier (2 for noisy surfaces) define the outliers which are removed from the model. The *Outlier Removal* resolution should be the same as that in the subsequent *Fusion* algorithm that generates a polygon mesh. The "fast" version of the *Fusion* algorithm is recommended by the manufacturer for Eva scans and large datasets. This algorithm triangulates the points within an average point to point distance or resolution, defined as 0.5 mm for the Eva scanner. The polygon mesh is further processed with the *Mesh Simplification* algorithm which reduces the size of the polygon mesh optimising the model to a predetermined accuracy or maximum deviation from the original mesh. An accuracy of 1 mm was adopted for this study as a suitable compromise between accuracy and memory requirements. Finally, the *Texturing* algorithm applies colour information to the polygon mesh for which a 512x512 resolution was adopted to ensure the quality of the resulting texture and maintain a manageable file size. A summary of the post-processing algorithms and parameters adopted are listed in Table 2 and the final polygon mesh model (obj) [47] of a typical bamboo pole is shown in Figure 6.

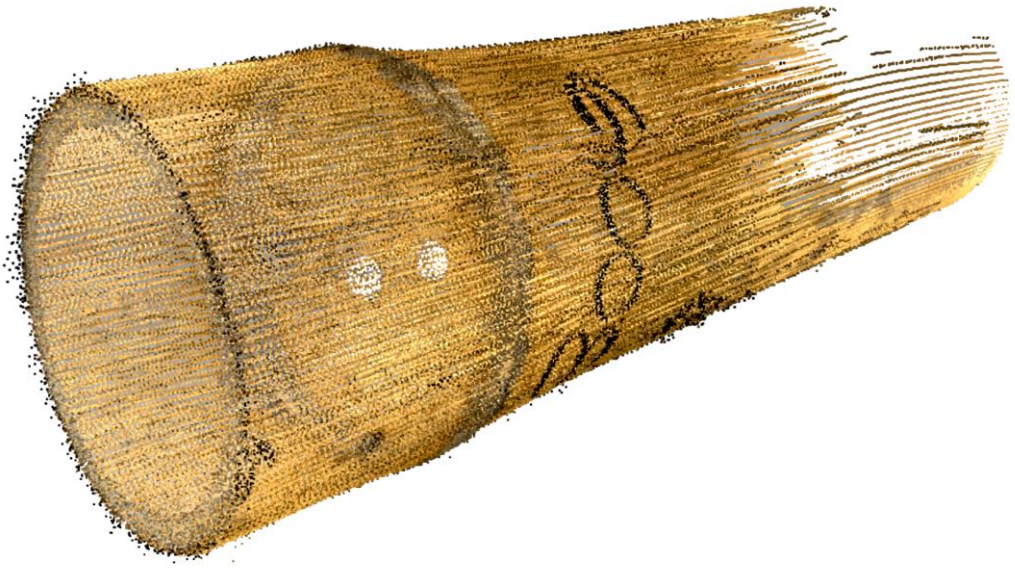

Figure 5. Scanned raw data of the end section of a bamboo pole

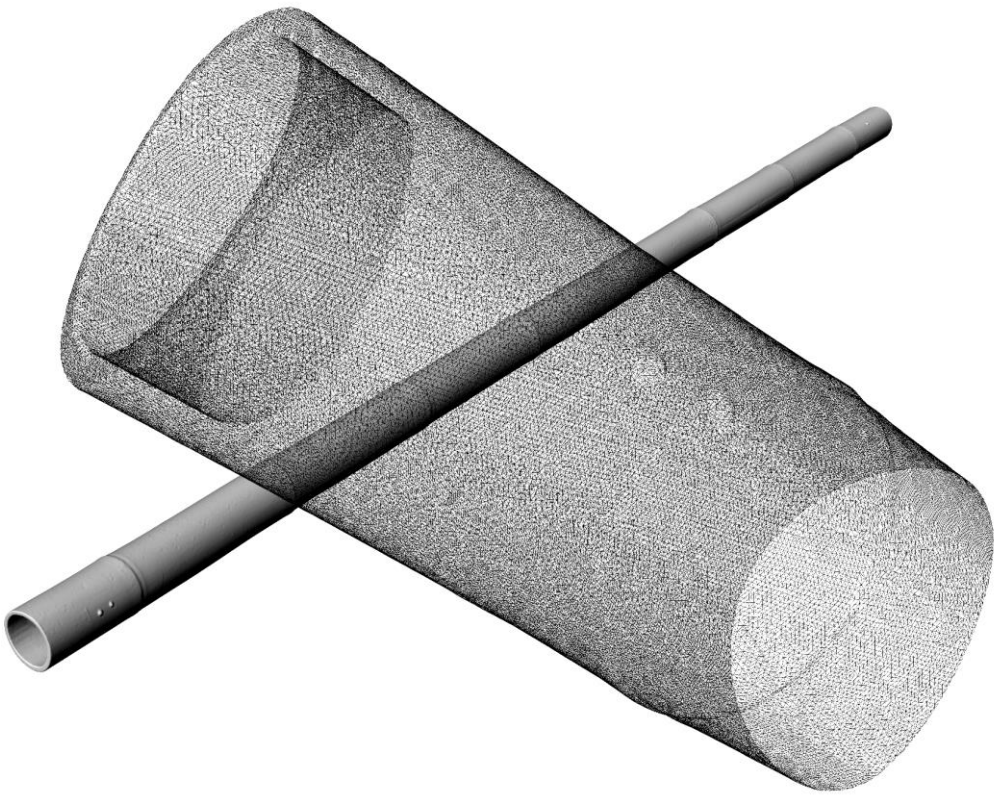

Figure 6. Rendered polygon mesh model of a bamboo pole and detail of its end section

Table 2. Post-processing algorithms and parameters in Artec Studio 12 [45]

Algorithm	Function	Parameters
1. Fine Registration	Alignment of captured frames	• Registration_algorithm: Geometry_and_Texture • Loop_closure: On
2. Global Registration	Optimisation of frame positions	• Registration_algorithm: Geometry_and_Texture
3. Outlier Removal	Elimination of outliers and noise	• Std_dev_mul_threshold: 2 • Resolution: 0.5 mm
4. Fusion (Fast)	Creation of polygonal 3D model	• Resolution: 0.5 mm
5. Mesh simplification	Reduction of number of polygons	• Accuracy: 1mm
6. Texture	Projection of textures onto mesh	• Texturing for: Export • Enable texture normalization: On • Output texture size: 512×512
7. Export	Export polygon mesh	• Mesh format: obj • Texture format: png

The resulting Artec Studio 12 project file size for an average 4 m long, 100 mm diameter pole is 2 GB and that of the corresponding exported obj mesh around 50 MB (75 MB with texture). The average mesh processing time was 7 minutes based on the standard hardware adopted for this study, but shorter processing times could be achieved in an industrial setting. The use of this mesh in any structural application would be impractical due to its large file size and lack of explicit geometric information. This mesh is therefore adopted as the basis to develop a much lighter NURBS model and a text-based database of geometric properties extracted from it.

2.4. NURBS model and text database

A bespoke Rhino.Python [48] script was developed to create a NURBS surface model much smaller in file size and more flexible than the polygon mesh (obj) of the 3D scanned poles. This script uses the large function library in Rhino3D [49] to generate this NURBS surface and discretise, extract and calculate all the relevant geometric properties of the poles. The processing of the polygon mesh starts with the identification of the position of all bamboo nodal diaphragms (nodes) and reference markers (i.e. M5 socket screws) through the analysis of the angle between normal vector of the mesh faces in the model. The mesh faces that form the relatively flat bamboo surface within an internodal region are almost parallel and therefore the angle between their normal vectors is close to zero. On the contrary, there is a well-defined angle between the mesh faces around both the characteristic circumferential nodal ridges on the bamboo surface and the raised reference markers. The angle between the normal vectors of these mesh faces ranges from approximately 10 to 20° for the adopted mesh density (Table 2) and thus it is possible to isolate them from the rest of the mesh. Figure 7a shows a render of a section of a typical polygon mesh model (obj) together with the extracted vertices of the mesh faces defining the nodal regions and the reference markers. Rectangular planes fit through these mesh vertices define the nodal planes of the pole while the position of each reference marker is determined by the centroidal point of the corresponding mesh vertices as shown in Figure 7b.

Sections are also extracted from the mesh at both ends of the poles and include both the outer an inner bamboo mesh surfaces captured at the start and end of the scanning process. Figure 7b shows the cross sections extracted from the polygon mesh at the bottom end of the pole together with the nodal cross sections of the external bamboo surface obtained from the intersection between the rectangular nodal planes and the mesh. The centroids of these nodal sections and those of the external sections at the pole ends define the centroidal axes of the external surface of the model shown in Figure 7b. Further sections parallel to the nodal planes and perpendicular to this centroidal axes are extracted from the mesh at the nodes and internodes respectively. In order to capture all relevant pole features, these sections are spaced 2mm apart and extend over a distance of approximately one pole diameter centred on the nodes and half a pole diameter centred on the middle of the internode as shown in Figure 7b. These sections are highly irregular and therefore modelled as Non-uniform rational B-splines (NURBS) whose shapes are determined by a series of control points [50]. The number of control points of each extracted NURBS section is limited to 20 as this significantly reduces the complexity of the model without affecting its accuracy. A surface is subsequently fit through all the external NURBS to create the bamboo exterior. Previous studies [14,16,20] have confirmed a linear variation in the wall thickness of bamboo poles along their length. Based on these findings, a second surface is fit through the two internal sections at the ends of the poles following the centroidal axes in Figure 7b. These external and internal surfaces constitute the final NURBS model of the bamboo pole shown in Figure 7c which includes the final position of the reference markers obtained by projecting the centroidal points of the initial mesh vertices onto the external bamboo surface.

The file size of the final NURBS model of a typical 4m pole is approximately 1MB (compared to a mesh file size of 50MB) and the distance between its outer surface and the corresponding vertices of the original mesh is less than 0.1mm in average. The compact file size and flexibility of NURBS models of bamboo poles make them suitable for their efficient use in digital modelling and fabrication processes for structural applications.

The final stage of the post-processing involves extracting all relevant geometric properties from this NURBS model in order to build a suitable database of each pole for structural modelling. The internodes at both ends of the pole which contain the reference

markers are considered sacrificial and thus excluded from this database. The cross sections at the nodes of the pole are found intersecting the rectangular nodal planes in Figure 7b and both the internal and external NURBS surfaces. These cross sections conservatively ignore the solid internal diaphragms that divide adjacent internodes and their centroids define the true centroidal axis of the pole. The growth pattern of bamboo [4,51] produces a series of relatively straight and prismatic internodes with significant changes of direction occurring at the nodes where they join adjacent internodes. This anatomic feature is the basis for the proposed structural discretisation of bamboo in which the overall geometry of a pole is defined by the centroids of its nodal sections while the geometric properties of the cross section at the centre of each internode are assigned to that entire internode. These internodal sections are normal to the centroidal axis as shown in Figure 7d along with the nodal cross sections and centroidal points extracted from the NURBS model. A typical internodal section and its corresponding equivalent circular tube are shown in Figure 8 together with the position of the arbitrary centroidal axes *y* & *z* as well as the section principal axes *1* & *2* and their orientation angle, θ. The properties of each internodal section considering both an equivalent circular tube and its actual asymmetric geometry are calculated as follows:

Cross sectional area, $A = A_o - A_i$ (1)

Equivalent outer diameter, $D = \sqrt{\frac{4A_o}{\pi}}$ (2)

Equivalent thickness, $t = \frac{D - \sqrt{D^2 - \frac{4A}{\pi}}}{2}$ (3)

Equivalent moment of inertia, $I = \frac{\pi}{64}[D^4 - (D - 2t)^4]$ (4)

Equivalent polar moment of inertia, $J = \frac{\pi}{64}[D^4 - (D - 2t)^4]$ (5)

Principal moments of inertia, $I_{1,2} = \frac{1}{2}\left[(I_y + I_z) \pm \sqrt{(I_z - I_y)^2 + 4I_{yz}^2}\right]$ (6)

Direction of principal moments of inertia, $\theta = \frac{1}{2} tan^{-1}\left(\frac{2I_{yz}}{I_z - I_y}\right)$ (7)

where: Ao and Ai are the cross-sectional areas of the outer and inner pole surfaces respectively and Iy, Iz and Iyz are the moments of inertia and product moment of inertia of the actual internodal cross section. These five properties are calculated directly from the NURBS model using the relevant Rhino3D function library. The processing time required to obtain a NURBS model and all relevant geometric properties of a typical 4 m long pole is approximately 5 minutes which could be further reduced in an industrial setting depending on the level of automation and available hardware. The properties of an equivalent circular tube [22] can be very powerful aids during the preliminary stages of a project, but the formal design, analysis and fabrication of bamboo structures require the use of the actual geometric properties of the poles to ensure their reliability and quality.

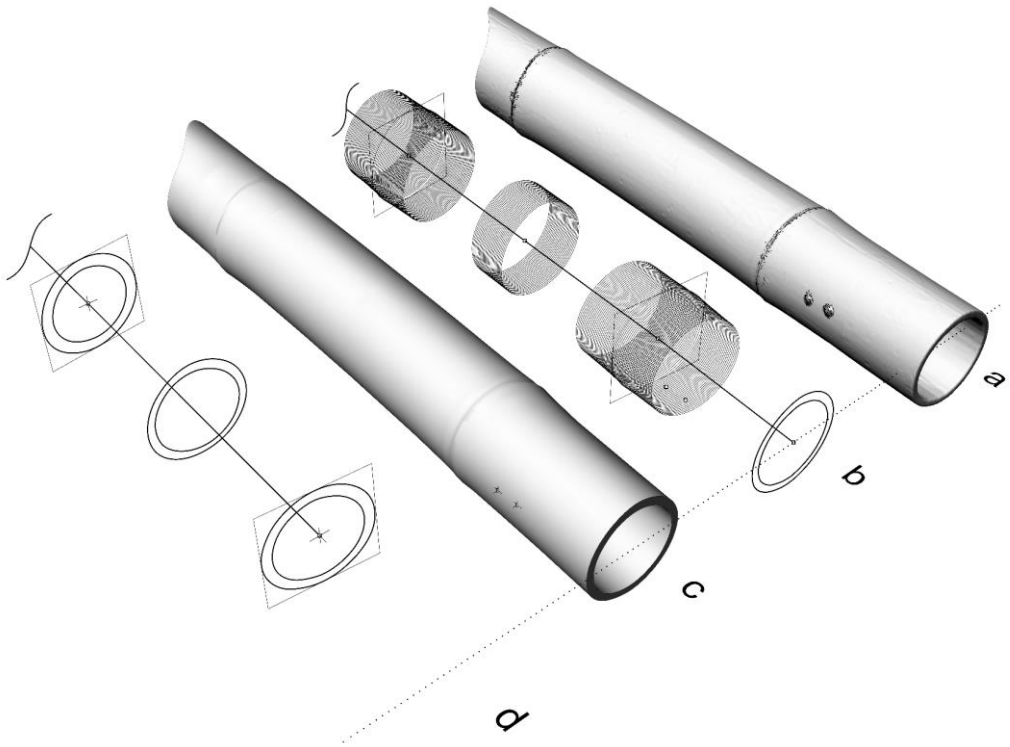

Figure 7. Development of the NURBS model of a bamboo pole and its structural discretisation

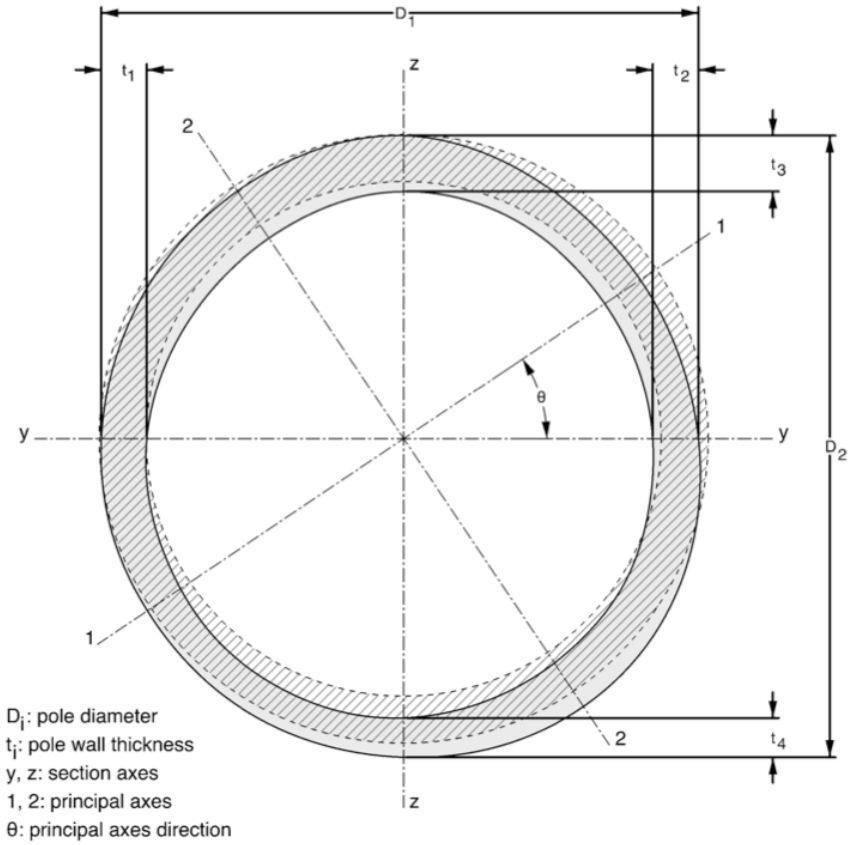

Figure 8. Cross section of bamboo and equivalent circular tube idealisation (hatched)

3. Validation

The developed digitisation process for bamboo poles was validated through its practical implementation on approximately 230 individual poles with a combined length of 500 m. Three bamboo species from different geographic regions were used to confirm the capability of the digitisation process to handle varying geometric features such as colour, texture, shape and size (Table 3).

Table 3. Details of bamboo samples

Species	Origin	Age (years)	Treatment	Avg. Diameter (mm)
Phyllostachys pubescens (Moso)	Jiangsu, P.R.China	3 - 4	Carbonisation/ Env. chamber	85
Guadua angustifolia kunth (Guadua)	Valle del Cauca, Colombia	2 - 5	Leaching/ Air-dried	110
Bambusa oldhamii (Oldhamii)	Veracruz, Mexico	3 - 5	Leaching/ Air-dried	65

The basic dimensions of approximately 15% of the scanned poles were hand-measured following ISO 22157-1-2004 [22] and included diameter, thickness and length. As shown in Figure 8, two diameters, D_1 and D_2, and four thicknesses, t_1, t_2, t_3 and t_4, were measured on each pole end-section with a Vernier calliper and compared with the corresponding dimensions on the digital model of the pole using the reference markers (Figure 2, Figure 7c) to locate their precise position. The length of the poles was measured as the distance between these reference markers at both ends of the pole. In addition, some selected poles were cut in half to measure their properties and confirm the assumption of a linear thickness variation along the length of the poles.

The average relative difference in the measurements of diameter and thickness between the physical poles and their digital models was approximately 3% in accordance with the scanner resolution of 0.5 mm. An average correlation factor, R^2, of 0.92 was obtained from linear regression analyses of the average section thicknesses at the ends and middle of each pole. This high correlation factor confirms the suitability of linearly interpolating the captured cross sections at the ends of the poles to model the internal surface of the bamboo wall. Also, the pole lengths extracted from the digital models were within $1/1000^{th}$ of the measured length on the physical poles. The accuracy achieved in the scanning process is in line with the general requirements for reverse engineering in buildings [52]. Also, compared to a manual measurement process, a similar but more consistent level of accuracy can be achieved through the digitisation of bamboo poles and it is estimated that a complete digital model of a bamboo pole can be generated in the time that would take a skilled operative to collect the basic measurements of only a few discrete sections along the pole.

A fundamental geometric property not covered in ISO 22157-1-2004 [22] is the out-of-straightness of the poles which can have significant implications on the structural behaviour [20] and buildability of bamboo structures. The complexity of manually measuring out-of-straightness is evident from the methods developed by Ghavami & Moreira [20] and Richard [21] as bamboo poles are highly irregular without any clear reference features. This irregularity is illustrated in Figure 9, which shows the longitudinal cross section of a digital model of a doubly-curved 3.2m long bamboo pole and its centroidal axis, against a reference horizontal line (dashed). The spatial information contained in these digital models can be used to efficiently quantify not only the out-of-straightness for any section of a pole but also all other information necessary to support the efficient and accurate selection, geometric modelling and numerical analysis of bamboo poles in building projects.

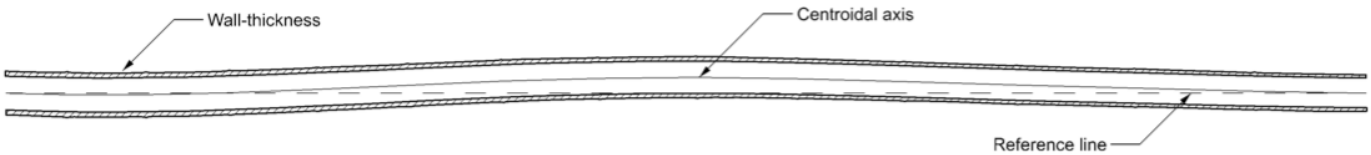

Figure 9. Longitudinal cross-section of a bamboo pole with double curvature

4. Case study

A small structural bamboo prototype was developed and assembled at the campus of the National University of Mexico (UNAM) based on a general geometric surface conceived by staff and students of UNAM Faculty of Architecture. This surface was used as the basis to form a system of reciprocal frame modules using the digitised Oldhamii bamboo poles previously described (Figure 10). In its simplest form, a reciprocal frame (RF) is a spatial arrangement of mutually supporting sloping beams placed in a closed circuit tangentially around a central point of symmetry [53]. Joining individual reciprocal frame units of predetermined geometry and topology can generate reciprocal frame grids that closely follow spatial surfaces of various morphologies as explored by [54–56] among others.

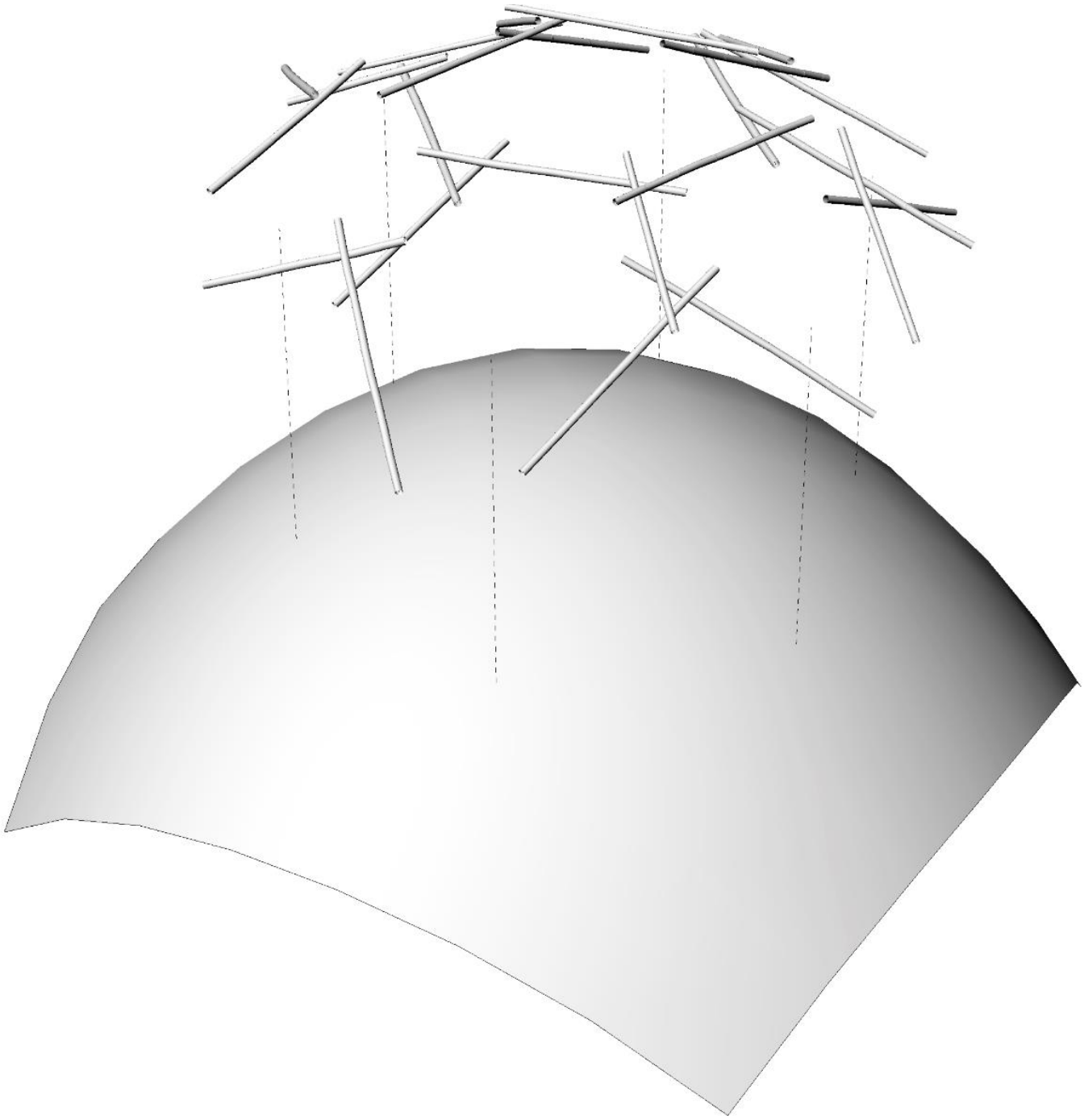

Figure 10. Basic surface and the respective reciprocal frame arrangement

A reciprocal frame grid was adopted for this case study as a potential structural system suitable for bamboo as short poles can be used to span long distances and their connections are limited to only two poles at any location within the structure. However, reciprocal frame grids completely rely on the accurate geometric modelling and assembly of their constituent parts and therefore, the digitisation of bamboo poles is fundamental to enable the use of these irregular and organic elements in this structural system. A computational method developed by the authors was used to determine the basic geometry of the reciprocal frame grid based on straight line elements with the eccentricity between them represented by a connector line perpendicular to both elements located at two position within each pole (Figure 11, top). The NURBS models of selected bamboo poles were imported into a digital model of the structure to locate them within the reciprocal frame grid. These digital pole models were positioned along and rotated about the corresponding line elements in the reciprocal frame grid to achieve the minimum deviation between their winding centrelines and the theoretical straight-line elements of the grid. The exact position of the reciprocal frame connectors on each bamboo pole was determined from the digital model as shown in Figure 11 along with the final digital model of one of the reciprocal frame units.

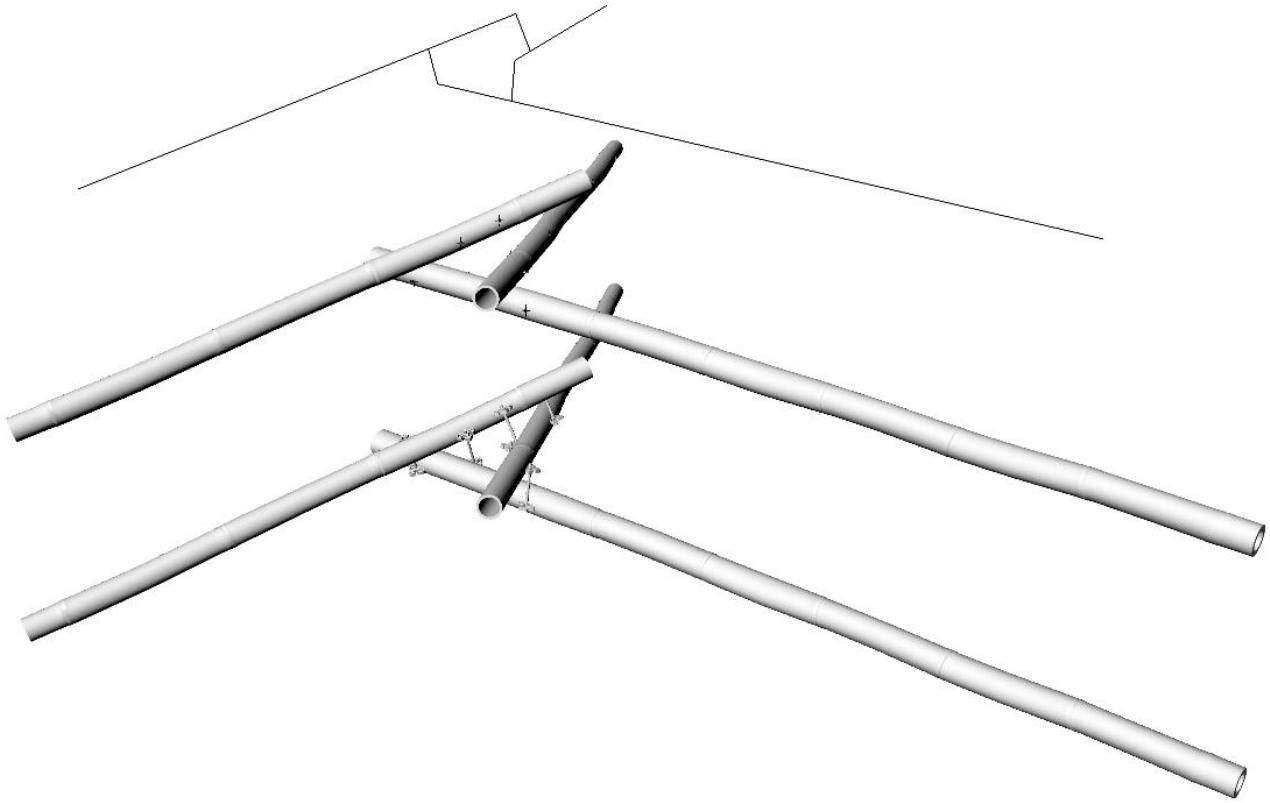

Figure 11. Development of the digital model of a single reciprocal frame unit

This exercise was solely focused on achieving the required prototype geometry and so simple connectors were used consisting of short triangular aluminium extrusions connected through M8 threaded bars and tied to each bamboo pole with steel banding (Figure 12). The length of each threaded bar defines the eccentricity between each pair of poles given by the connector line of the reciprocal frame grid (Figure 11, top). The digital information contained within the model of this structure provides the basis to perform further analysis (e.g. structural, optimisation, etc) and integrate this model into Building Modelling Information platforms.

Figure 12. Reciprocal frame connectors

The assembly process of this prototype consisted in extracting the exact location of each connector from the digital model and translating it into the corresponding physical pole using the scanning markers shown in Figure 2 as reference. Individual reciprocal frame units were built sequentially and finally joined together through their common elements as shown in Figure 13. The completed prototype is shown in Figure 14. The as-built geometry of this prototype was determined using a laser distance measurer Leica Disto 910 Pro, with an accuracy of ±2 mm/10 m, showing an average discrepancy with the overall geometry of the digital model of approximately 20 mm. This discrepancy is comparable to the ±5 mm (±10 mm for storey plumb) tolerance usually adopted for standard timber frame construction [57] with the difference likely to be due to the geometric complexity of the reciprocal frame system and small differences in ground levels which were only approximately defined using the Leica Disto 910 Pro.

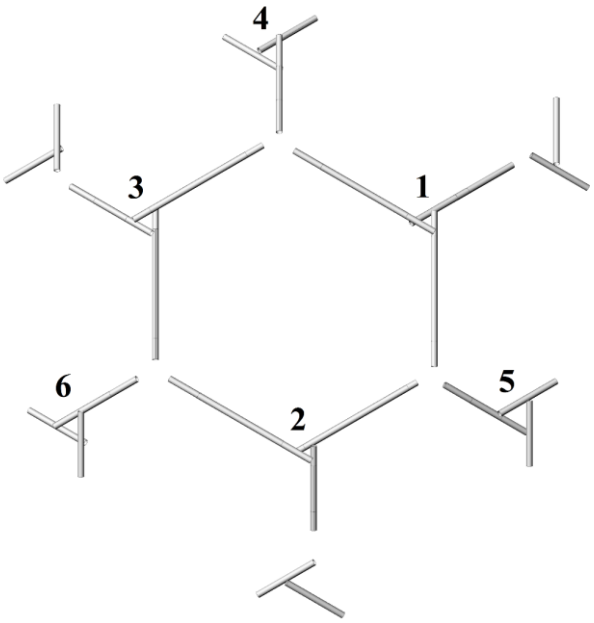

Figure 13. Construction sequence of reciprocal frame units

Figure 14. Bamboo reciprocal frame prototype

5. Conclusions

This paper presents the details of a 3D scanning and post-processing workflow for the digitisation of bamboo poles with the aim of managing the inherent geometric variability of this natural structural element. This workflow is based on the use of an entry-level structured-light 3D scanner to acquire the poles' geometry and texture together with a bespoke computer script developed to convert the captured polygon mesh into a light and flexible NURBS model. The key parameters used in the scanning process are presented as the basis for its potential implementation in an industrial setting. The digitisation of over 230 poles with a combined length of 500 m was completed confirming the high accuracy of the final geometric (NURBS) models which showed an average dimensional difference of 3% compared with manual physical measurements. In addition, the discretisation of these models to produce numerical databases of cross-sectional properties required for the formal structural analysis of bamboo structures are discussed. A case study of a reciprocal frame structure is presented to show the potential of digital models to support the exploration and development of alternative structural solutions for bamboo poles that would be otherwise impractical to implement due to the organic nature and irregularity of the material. The as-built geometry of this reciprocal frame structure showed an average difference with its digital model of approximately 20 mm which is comparable to the tolerances usually adopted for standard timber frame construction.

The digital representation of bamboo poles as building elements together with a complete description of their geometric properties is intended to lay the foundations to support the integration of bamboo poles in modern Building Information Modelling (BIM) platforms. This integration can provide the construction industry with the necessary support to design, build and maintain high quality structures that incorporate this sustainable and renewable resource. Bamboo poles provide an ideal opportunity to adopt modern technologies in the development of automated processes that are not only focused on their transformation into industrialised products but on the non-destructive characterisation of these natural structural elements at zero environmental cost.

6. Acknowledgements

The work presented in this paper was supported by the UK Engineering and Physical Sciences Research Council (EPSRC) (Grant Nos: EP/M017702/1 & EP/P510890/1). The authors would like to thank Dr Gerardo Oliva-Salinas, Dr David Trujillo and Dr Li Haitao for enabling the on-site activities and procurement of the bamboo samples used in this study as well as Dr Chuhee Lee and Martha Godina for their support during the implementation of the 3D scanning workflow and development of the prototype.

7. References

[1] UN-Habitat, 53 UN-Habitat Model Projects, Nairobi, Kenya, 2013.

[2] J. Allwood, J. Cullen, Sustainable Materials – with Both Eyes Open: Future Buildings, Vehicles, Products and Equipment, UIT Cambridge Ltd, Cambridge, UK, 2011.

[3] D. Grosser, W. Liese, On the anatomy of Asian bamboos, with special reference to their vascular bundles, Wood Sci. Technol. 5 (1971) 290–312. doi:10.1007/BF00365061.

[4] W. Liese, Research on bamboo, Wood Sci. Technol. 21 (1987) 189–209.

[5] E. Zea Escamilla, G. Habert, Environmental impacts of bamboo-based construction materials representing global production diversity, J. Clean. Prod. 69 (2014) 117–127. doi:10.1016/j.jclepro.2014.01.067.

[6] W. Wu, Q. Liu, Z. Zhu, Y. Shen, Managing Bamboo for Carbon Sequestration, Bamboo Stem and Bamboo Shoots, Small-Scale For. 14 (2015) 233–243. doi:10.1007/s11842-014-9284-4.

[7] S. Brown, Present and potential roles of forests in the global climate change debate, Unasylva. (1996) 3–10. http://www.fao.org/docrep/w0312e/w0312e03.htm#present and potential roles of forests in the global climate change debate.

[8] M.S. Vorontsova, L.G. Clark, J. Dransfield, R. Govaerts, T. Wilkinson, W.J. Baker, World checklist of bamboos and rattans, International Network for Bamboo and Rattan, Beijing, China, 2016. http://apps.kew.org/wcsp.%0AHow.

[9] S. Kaminski, A. Lawrence, D. Trujillo, Structural use of bamboo Part 1 : Introduction to bamboo, Struct. Eng. (2016) 40–43.

[10] I.R. Hunter, Bamboo — solution to problems, J. Bamboo Ratt. 1 (2002) 101–107.

[11] J. Janssen, Designing and Building with Bamboo, 2000.

[12] BS EN 336, British adoption of European Standard BS EN 336: 2013. Structural timber - Sizes, permitted deviations, (2013).

[13] J. Li, Y. Yuan, X. Guan, Assessing the Environmental Impacts of Glued-Laminated Bamboo Based on a Life Cycle Assessment, BioResources. 11 (2016) 1941–1950. doi:10.15376/biores.11.1.1941-1950.

[14] S. Amada, Y. Ichikawa, T. Munekata, Y. Nagase, H. Shimizu, Fiber texture and mechanical graded structure of bamboo, Compos. Part B Eng. 28 (1997) 13–20. doi:10.1016/S1359-8368(96)00020-0.

[15] K.F. Chung, W.K. Yu, Mechanical properties of structural bamboo for bamboo scaffoldings, Eng. Struct. 24 (2002) 429–442. doi:10.1016/S0141-0296(01)00110-9.

[16] T.S.S. Paraskeva, G. Grigoropoulos, E.G.G. Dimitrakopoulos, Design and experimental verification of easily constructible bamboo footbridges for rural areas, Eng. Struct. 143 (2017) 540–548. doi:10.1016/j.engstruct.2017.04.044.

[17] D. Trujillo, S. Jangra, J.M. Gibson, Flexural properties as a basis for bamboo strength grading, Proc. Inst. Civ. Eng. - Struct. Build. 170 (2017) 284–294. doi:10.1680/jstbu.16.00084.

[18] Nurmadina, N. Nugroho, E.T. Bahtiar, Structural grading of Gigantochloa apus bamboo based on its flexural properties, Constr. Build. Mater. 157 (2017) 1173–1189. doi:10.1016/j.conbuildmat.2017.09.170.
[19] L.J. Gibson, M.F. Ashby, G.N.N. Karam, U. Wegst, H.R. Shercliff, The Mechanical Properties of Natural Materials. II. Microstructures for Mechanical Efficiency, Proc. R. Soc. A Math. Phys. Eng. Sci. 450 (1995) 141–162. doi:10.1098/rspa.1995.0076.
[20] K. Ghavami, L.E. Moreira, The influence of initial imperfections on the buckling of bamboo columns, Asian J. Civ. Eng. (Buillding Housing). 3 (2002) 1–16.
[21] M. Richard, Assesing the performance of bamboo sturctural components, University of Pittsburgh, 2013.
[22] ISO 22157-1, International Standard Organization ISO 22157-1. Bamboo-Determination of physical and mechanical properties- Part 1: Requirements, (2004).
[23] G. Moustakides, D. Briassoulis, E. Psarakis, E. Dimas, 3D image acquisition and NURBS based geometry modelling of natural objects, Adv. Eng. Softw. 31 (2000) 955–969. doi:10.1016/S0965-9978(00)00060-0.
[24] J. Miles, M. Pitts, H. Pagi, G. Earl, New applications of photogrammetry and reflectance transformation imaging to an Easter Island statue, Antiquity. 88 (2014) 596–605. doi:10.1017/S0003598X00101206.
[25] C. Nicolae, E. Nocerino, F. Menna, F. Remondino, Photogrammetry applied to problematic artefacts, in: Int. Arch. Photogramm. Remote Sens. Spat. Inf. Sci. - ISPRS Arch., Garda, Italy, 2014: pp. 451–456. doi:10.5194/isprsarchives-XL-5-451-2014.
[26] J. Martinez-Llario, E. Coll, J. Herraez, Three-diemensional scanner software using a video camera, Adv. Eng. Softw. 37 (2006) 484–489. doi:10.1016/j.advengsoft.2005.08.003.
[27] N.J. Shih, H.J. Wang, C.Y. Lin, C.Y. Liau, 3D scan for the digital preservation of a historical temple in Taiwan, Adv. Eng. Softw. 38 (2007) 501–512. doi:10.1016/j.advengsoft.2006.09.014.
[28] W. Bin Yang, M. Bin Chen, Y.N. Yen, An application of digital point cloud to historic architecture in digital archives, Adv. Eng. Softw. 42 (2011) 690–699. doi:10.1016/j.advengsoft.2011.05.005.
[29] P. Fechteler, P. Eisert, Adaptive color classification for structured light systems, in: 2008 IEEE Comput. Soc. Conf. Comput. Vis. Pattern Recognit. Work., IEEE, 2008: pp. 1–7. doi:10.1109/CVPRW.2008.4563048.
[30] J.-H. Jeon, I.-D. Jung, J.-H. Kim, H.-Y. Kim, W.-C. Kim, Three-dimensional evaluation of the repeatability of scans of stone models and impressions using a blue LED scanner, Dent. Mater. J. 34 (2015) 686–691. doi:10.4012/dmj.2014-347.
[31] G. Castellazzi, A.M. D'Altri, G. Bitelli, I. Selvaggi, A. Lambertini, From laser scanning to finite element analysis of complex buildings by using a semi-automatic procedure, Sensors (Switzerland). 15 (2015) 18360–18380. doi:10.3390/s150818360.
[32] 3DReshaper, (2019). https://www.3dreshaper.com/en/software-en/ (accessed January 24, 2019).
[33] Cloud Compare, (2019). https://www.danielgm.net/cc/ (accessed January 24, 2019).
[34] MeshLab, (2019). http://www.meshlab.net/ (accessed January 24, 2019).
[35] L. Barazzetti, F. Banfi, R. Brumana, G. Gusmeroli, D. Oreni, M. Previtali, F. Roncoroni, G. Schiantarelli, BIM From laser clouds and finite element analysis: combining structural analysis and geometric complexity, ISPRS - Int. Arch. Photogramm. Remote Sens. Spat. Inf. Sci. XL-5/W4 (2015) 345–350. doi:10.5194/isprsarchives-XL-5-W4-345-2015.
[36] R. Bénière, G. Subsol, G. Gesquière, F. Le Breton, W. Puech, A comprehensive process of reverse engineering from 3D meshes to CAD models, CAD Comput. Aided Des. 45 (2013) 1382–1393. doi:10.1016/j.cad.2013.06.004.
[37] P. Benko, R.R. Martin, T. Várady, Algorithms for reverse engineering boundary representation models, CAD Comput. Aided Des. 33 (2001) 839–851. doi:10.1016/S0010-4485(01)00100-2.
[38] B. Conde, A. Villarino, M. Cabaleiro, D. Gonzalez-Aguilera, Geometrical issues on the structural analysis of transmission electricity towers thanks to laser scanning technology and finite element method, Remote Sens. 7 (2015) 11551–11569. doi:10.3390/rs70911551.
[39] T. Hinks, H. Carr, L. Truong-Hong, D.F. Laefer, Point Cloud Data Conversion into Solid Models via Point-Based Voxelization, J. Surv. Eng. 139 (2013) 72–83. doi:10.1061/(ASCE)SU.1943-5428.0000097.
[40] R. Garber, BIM Design: Realising the creative potential of building information modelling, John Wiley and Sons, West Sussex, UK, 2014.
[41] National BIM Standard-US, (2018). http://www.nationalbimstandard.org/ (accessed October 1, 2018).
[42] Wikipedia, Polygon Mesh, (2019). https://en.wikipedia.org/wiki/Polygon_mesh (accessed January 24, 2019).
[43] Wikipedia, Non-uniform rational S-spline, (2019). https://en.wikipedia.org/wiki/Non-uniform_rational_B-spline (accessed January 24, 2019).
[44] R. Lorenzo, C. Lee, J.G. Oliva-Salinas, M.J. Ontiveros-Hernandez, BIM Bamboo: a digital design framework for bamboo culms, Proc. Inst. Civ. Eng. - Struct. Build. 170 (2017) 295–302. doi:10.1680/jstbu.16.00091.
[45] Artec 3D, (2019). https://www.artec3d.com/ (accessed January 24, 2019).
[46] C. Bernal, B. De Agustina, M.M. Marín, A.M. Camacho, Performance evaluation of optical scanner based on blue LED structured light, Procedia Eng. 63 (2013) 591–598. doi:10.1016/j.proeng.2013.08.261.
[47] Wikipedia, Wavefront .obj file, (2019). https://en.wikipedia.org/wiki/Wavefront_.obj_file (accessed January 24, 2019).
[48] Rhino Developer Docs, (2019). https://developer.rhino3d.com/api/RhinoScriptSyntax/ (accessed January 24, 2019).
[49] RMNA, Robert McNeel & Associates- Rhinoceros 3D. Software Version 5.0, (2015).
[50] G.E. Farin, NURBS: From projective geometry to practical use, A.K. Peters, Ltd, Natick, MA, USA, 1999.
[51] D. Taylor, B. Kinane, C. Sweeney, D. Sweetnam, P. O'Reilly, K. Duan, The biomechanics of bamboo: investigating the role of the nodes, Wood Sci. Technol. 49 (2015) 345–357. doi:10.1007/s00226-014-0694-4.
[52] H. Runne, W. Niemeier, F. Kern, Application of Laser Scanners to Determine the Geometry of Buildings, in: Opt. 3D Meas.

Tech. IV, Wien, 2001: pp. 41–48.
[53] O. Popovic Larsen, Reciprocal Frame Architecture, Elsevier Ltd, Oxford, UK, 2008. https://casaeco.files.wordpress.com/2012/03/reciprocal-frame-architecture.pdf (accessed January 24, 2019).
[54] O. Baverel, M. Saidani, The multi-reciprocal grid system, J. Int. Assoc. Shell Spat. Struct. 40 (1999) 33–41.
[55] C. Douthe, O. Baverel, Design of nexorades or reciprocal frame systems with the dynamic relaxation method, Comput. Struct. 87 (2009) 1296–1307. doi:10.1016/j.compstruc.2009.06.011.
[56] P. Henning, M. Sassone, A. PUGNALE Assistant Professor, D. PARIGI Assistant Professor, P.H. KIRKEGAARD Professor, M. SASSONE Assistant Professor, The Principle of Structural Reciprocity The principle of structural reciprocity: history, properties and design issues, (2015).
[57] R. Lancashire, L. Taylor, Timber Frame Construction, TRADA Technology Ltd., High Wycombe, 2011.